

# ADVANCES IN MECHANISM OF CLEAVAGE FRACTURE AT LOW TEMPERATURE: PART I. CRITICAL EVENT

J.H. CHEN and C. YAN

Welding Research Institute, Gansu University of Technology,  
Lanzhou 730050, Gansu, P.R. China

## ABSTRACT

The critical event of cleavage fracture at low temperature is considered as the most difficult step in the process from initiation to propagation of a cleavage crack. In this study, it has been found that the critical event are different in the notched and precracked specimens, even for a C-Mn weld steel. In the notched specimens, the critical event are identified as the propagation of ferrite grain-sized microcracks into the neighboring matrixes and in the precracked specimens second phase particle-sized microcracks into the neighboring ferrite grains. The temperature has an influence on critical event. The reason of the variation of critical event can be related to the different sharpness at the tip of a notch and a precrack, which can cause different distributions of triaxiality and effective shear stress.

## KEYWORDS

Critical event; cleavage fracture stress; propagation; ferrite grain-sized microcrack; second phase particle-sized microcrack; triaxiality; effective shear stress

## INTRODUCTION

The critical event is considered as the most difficult step in the process of cleavage fracture from crack initiation to propagation. What is the critical event in cleavage fracture for C-Mn steel has been argued for many years. In 50-60's, based on the view of crack initiation resulting from a pile-up of dislocations, the critical event was considered as the propagation of a ferrite grain-sized microcrack into the neighboring grains. In 70-80's, however, according to Smith's equation (Smith, 1966), it was related to the propagation of second phase particle-sized microcrack into the ferrite grain. In previous works (Chen et al. 1990a, b, c, d and 1991), the authors have made a detailed investigation on the critical events. In the present article, a summary and a further analysis of those results are given.

## MATERIALS AND EXPERIMENTS

The materials used were C-Mn steel and C-Mn, Ti-B, and Ti-B-Ni weld metals with composition shown in Table 1.

Table 1. Composition of C-Mn steel and weld metals. (wt pct)

Materials	C	Mn	Si	S	P	Ti	B	Ni
C-Mn base steel	0.18	1.49	0.35	0.03	0.01	*	*	*
C-Mn weld metals	0.07	1.24	0.28	0.02	0.01	0.03	*	*
Ti-B weld metals	0.06	1.49	0.48	0.02	0.01	0.03	0.004	*
Ti-B-Ni weld metals	0.07	1.60	0.19	0.03	0.02	0.02	0.003	0.45

\* Not measured

The standard Charpy specimens with root radius  $\rho = 0.25\text{mm}$  were used (Chen et al., 1988). Three types of deep notched specimens for 4 point bending (4PB) tests, i.e., single notch (Griffith et al., 1971; Chen et al. 1990b,  $\rho = 0.25\text{mm}$ ), double notches (Chen et al., 1991,  $\rho = 0.25\text{mm}$ ) and single notch with different root radii ( $\rho = 0.05, 0.075, 0.15, 0.25, \text{ and } 0.35\text{mm}$ ) were adopted. Pre-cracked specimens for three point bending tests (COD) were used also.

The Charpy impact tests were made at  $-45^\circ\text{C}$  and  $-60^\circ\text{C}$  at a hammer speed of  $5\text{m/sec}$ . Most of 4PB tests were carried out at  $-196^\circ\text{C}$  and a part at  $-150^\circ\text{C}$ . The COD tests were made at  $-70^\circ\text{C}$ ,  $-110^\circ\text{C}$  and  $-196^\circ\text{C}$  and some of the COD specimens were unloaded at 95% fracture load. The cross-head speed of testing machine in both 4PB and COD tests was  $1\text{mm/min}$ .

Several metallographic sections as shown in Fig. 1a were sampled at a 4PB or a COD specimen to observe the remaining cleavage microcracks which were initiated but were shorter than critical length for unstable cleavage and remained in the specimens. Especially the remaining crack below the survived notch in the fractured double notches 4PB specimens and in the COD specimens unloaded prior to fracture were observed carefully. The microstructural units limiting the maximum length of remaining crack were defined as microstructural domain of critical event. The sizes of ferrite grains of the zone in which the cleavage crack initiated was measured by a special metallographic section, as shown in Fig. 1b. The relationships between the size of these grains or the maximum length of remaining crack and macro-mechanical properties were used to reveal the critical event. The fracture surfaces were observed in detail using a scanning electron microscope (SEM) and the size of second phase particles initiating the cleavage crack and the size of the cleavage facets were measured to give a supplement for determining the critical event. The local cleavage fracture stress  $\sigma_f$  can be evaluated with Charpy, 4PB and COD testing. The detailed methods were described in References (Chen et al., 1990a and c).

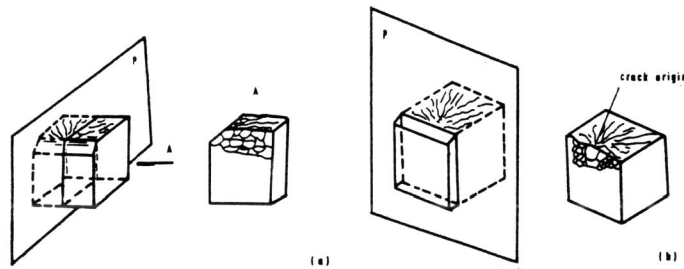


Fig. 1 Metallographic sections for examining; (a) remaining cracks, and (b) microstructure where cleavage crack initiated.

### EXPERIMENTAL RESULTS

The ferrite grain-sized remaining cracks were found in fractured Charpy specimens at  $-45^\circ\text{C}$  and  $-60^\circ\text{C}$ , as shown in Fig. 2a and the similar cracks were observed below the tip of survived notch in the double notched 4PB specimens at  $-150^\circ\text{C}$  also (Fig. 2b).

Furtherly, as shown in Fig. 3 the ferrite grain-sized cracks were observed in fractured 4PB specimens with different notch root radii.

In the COD specimens unloaded under 95% fracture load at  $-110^\circ\text{C}$ , only the second phase-sized remaining cracks were observed, as shown in Fig. 4. In the COD specimens unloaded at  $-70^\circ\text{C}$ , as the crack tip opening ( $\delta$ ) was small ( $< 20\mu\text{m}$ ), only the second phase-sized cracks were observed

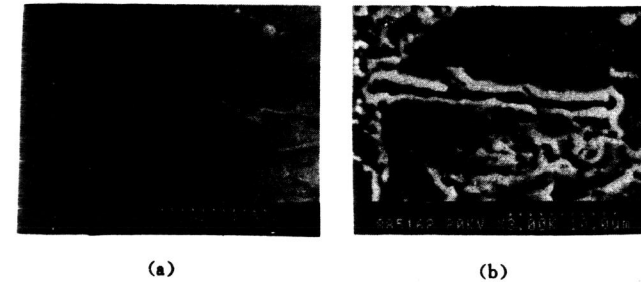


Fig. 2 Ferrite grain-sized cracks remaining in; (a) Charpy specimen at  $-60^\circ\text{C}$ , and (b) double notched 4PB at  $-150^\circ\text{C}$ .

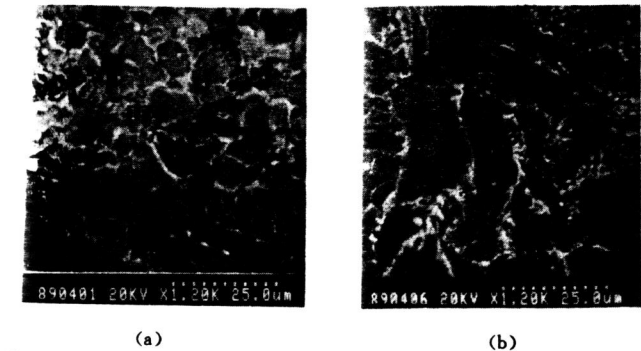


Fig. 3 Ferrite grain-sized remaining cracks in 4PB specimens with notch root radii; (a)  $\rho = 0.075\text{mm}$ , and (b)  $\rho = 0.25\text{mm}$ .

(Fig. 5a). But ferrite grain-sized cracks could be found when the  $\delta$  was wider ( $\delta = 25\mu\text{m}$ , Fig. 5b).

The statistical distribution of size of the remaining cracks in Charpy specimens at  $-65^\circ\text{C}$  and  $-60^\circ\text{C}$  and COD specimens at  $-110^\circ\text{C}$  are indicated in Fig. 6.

As shown in Fig. 7a and 7b, in Charpy specimens, there were apparent relationship between the Charpy absorbed energy and both the size of ferrite grains in the region of cleavage initiation (Fig. 7a) and the maximum length of remaining cracks (Fig. 7b). Additionally, in Fig. 8, the size of facets around the second-phase particle initiating the cleavage crack are related to the cleavage fracture stress  $\sigma_f$  measured in 4PB specimens.



Fig. 4 Second phase-sized remaining crack in COD specimen at  $-110^\circ\text{C}$

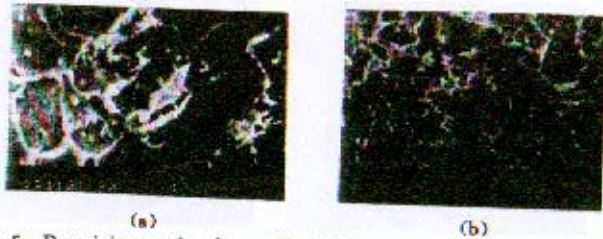


Fig. 5 Remaining cracks observed in COD specimens unloaded at  $-70^{\circ}\text{C}$ : (a)  $\delta < 20\mu\text{m}$ , and (b)  $\delta = 65\mu\text{m}$ .

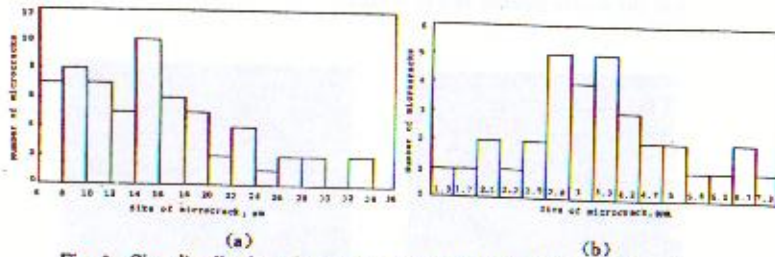


Fig. 6 Size distribution of remaining microcracks in: (a) notched specimens, and (b) COD specimens.

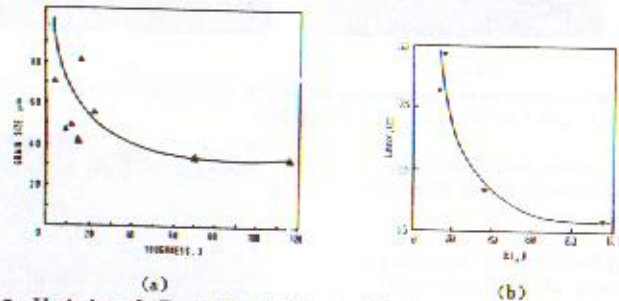


Fig. 7 Variation of  $\sigma_E - 60^{\circ}\text{C}$  with (a) size of ferrite grains in the region of cleavage initiation, and (b) the maximum length of remaining crack.

The cleavage fracture stress measured in notched and precracked specimens are shown in Table 2.

The statistical distribution of the size of second-phase particles which initiated the cleavage cracks are plotted in Fig. 9a and 9b.

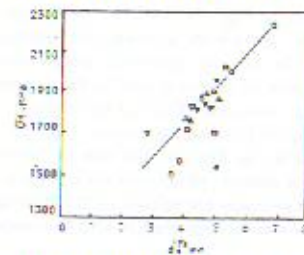


Fig. 8 Relationship between size of the facets and  $\sigma_f$ .

Table 2.  $\sigma_f$  measured in different specimens

Materials	temperature ( $^{\circ}\text{C}$ )	specimens	$\sigma_f$ (MPa)
C-Mn base steel	-45	Charpy	1494
	-140	4PB	1453
	-110	COD	2273
C-Mn weld metals	-45	Charpy	1726
	-143	4PB	1742
	-109	COD	2382
Ti-B weld metals	-68	Charpy	1840
	-140	4PB	1808
	-110	COD	2440

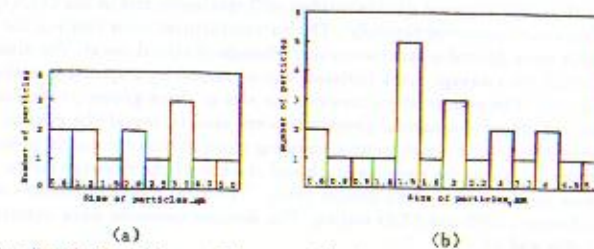


Fig. 9 Size distribution of second-phase particles initiating the cleavage fracture: (a) in 4PB specimens, and (b) in COD specimens.

## DISCUSSION

**Critical Event is Changeable.** Based on above results, it is obvious that the critical event were different in notched and precracked specimens. In other words, the sharpness of notch root has an influence on the critical event for the same material.

As indicated in Fig. 2 and Fig. 3 in the 4PB specimens with different root radii at different temperature and in Charpy specimens, the ferrite grain-sized cracks arrested in ferrite grains boundaries were observed. This fact revealed that the ferrite boundaries were main obstacle for unstable cleavage propagation. Therefore, the critical event here was considered as the propagation of a just-being formed ferrite grain crack into neighboring ferrite grains. A supplement evidence of above explanation can be obtained from the relationships between Charpy absorbed energy and both size of ferrite in the region of cleavage initiation (Fig. 7a) and size of the maximum remaining crack (Fig. 7b). In 4PB testing, as the size of cleavage facet was less than  $40\mu\text{m}$ , it has a definite relation with  $\sigma_f$  (Fig. 8) and this may be considered as another evidence. On the other hand, as the facet was more than  $40\mu\text{m}$ , the scatter of  $\sigma_f$  increased. It implied that the cleavage facet larger than  $40\mu\text{m}$  may be a result of unstable cleavage propagation.

In COD specimens unloaded at  $-110^{\circ}\text{C}$ , only the second phase-sized cracks were observed. It implies that the boundaries between ferrite and second phase is the main obstacle for cleavage propagation in precracked specimens. Therefore the critical event is the propagation of second phase particle sized crack into the neighboring ferrite grains, and it is consistent with some investigations carried out recently (Hahn, 1984).

For the COD specimens unloaded at  $-70^{\circ}\text{C}$ , as the crack tip opening was larger ( $65\mu\text{m}$ ), the ferrite grain sized remaining cracks were found. It is indicated furtherly that the sharpness of notch root is

the main factor to influence critical event. In addition, the testing temperature has an effect on the critical event also.

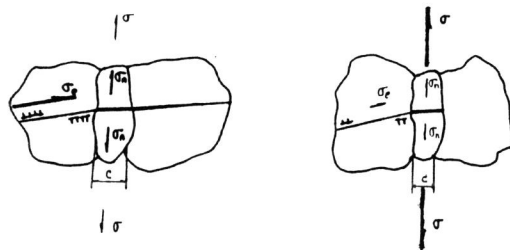
No remaining cracks were found in COD specimens fractured or unloaded at  $-196^{\circ}\text{C}$ . It reasonable to assume that the cleavage may be a crack initiation controlled process in precracked specimens at very low temperature.

**Variation of  $\sigma_f$  in Notched and Precracked Specimens.** As indicated in Table 2, the  $\sigma_f$  measured in notched specimen are about 600~800MPa lower than that in precracked specimen, and it can be understood in terms of the decrease of critical length of remaining crack from 30~40 $\mu\text{m}$  to 8 $\mu\text{m}$  (Fig. 6). In Hou's work (Hou et al. 1985) the variation of  $\sigma_f$  measured in notched and precracked specimens was attributed to the different high stress volume. In other words, there is a higher normal stress but a smaller high stress volume ahead of a precrack tip where the probability of sampling a largest "eligible" particles as a crack nucleus is smaller. If this view is right, the size of crack-initiating particles ahead of a precrack would be smaller than that ahead of a notch. But this was not the case, as shown in Fig. 9, no marked difference exists in the particles size distribution for two cases. Therefore, the reason of the variation of  $\sigma_f$  in notched and precracked specimens can be attributed to the variation of critical event (Fig. 6) instead of statistical effect induced by different high stress volumes.

**Reason of Variation of Critical Event in Notched and Precracked Specimen.** The variation of critical event can be explained in terms of the stress state ahead a precrack and a notch. As shown in Fig. 10, Stroh (Stroh, 1957) considered that the normal stress at a distance  $r$  ahead of a pile-up of dislocations induced by a effective shear stress  $\sigma_s$  could be expressed by :

$$\sigma_n = \sigma_s (L/r)^{1/2} \cdot f(\theta) \quad (1)$$

where the dislocations occupy a length  $L$  in the slip plane and  $f(\theta)$  is a angle factor. The maximum  $\sigma_n$  can be obtained at the plane which inclined  $70.5^{\circ}$  to the slip plane.



(a) notched specimen, low  $\sigma/\sigma_n$ . (b) precracked specimen, high  $\sigma/\sigma_n$ .  
Fig. 10 A proposed physical model for the variation of critical event.

In Fig. 10a, supposing the thickness of second phase, i. e.,  $C$  is equal to the  $r$ . In the event of forming a second phase-sized crack induced by pile-up of dislocations, the normal stress, at the boundary between the crack and ferrite grain, is the sum of applied normal stress  $\sigma$  and the additional stress  $\sigma_n$  expressed in Equation 1. Usually as the  $C$  is very small, the  $\sigma_n$  may play a important role during fracture.

In notched specimens, there are a lower triaxiality (i. e., a lower  $\sigma$ ) but a higher effective shear stress ( $\sigma_s$ ) below a notch root. The combination of  $\sigma$  and  $\sigma_s$  may enable the second phase particle-sized microcrack to propagate across the boundary and into neighboring ferrite grains. From Equation 1, the  $\sigma_n$  is decreased sharply with increasing the length of micro-crack. As a result, the microcrack may be arrested at the boundaries of ferrite due to insufficient applied normal stress. Therefore, the critical event is the propagation across the boundaries between ferrite grains.

Otherwise, there are a higher triaxiality, i. e., a higher ratio between  $\sigma$  and  $\sigma_s$  in precracked speci-

men. When the second phase particle-sized microcrack propagate into ferrite due to the combination of  $\sigma$  and  $\sigma_s$ , the  $\sigma$  is high enough to make a unstable propagation for the growing microcrack. Hence, it is impossible to find a ferrite grain-sized crack. The critical event is considered as the crack propagation across the boundaries between second phase and ferrite grains.

Because the surface energy in a grain is much less than that in grain boundary, once a microcrack cut through a boundary, it will propagate through whole grain. As a result, the change of the length of remaining crack is usually not continuous and it is in step with the size of second phase or ferrite. For example, in this study, the critical length steps from about 8 $\mu\text{m}$  in precracked specimen to 20~30 $\mu\text{m}$  in notched specimens.

With decreasing temperature, the dislocation friction stress  $\sigma_s$  is increased and therefore effective shear stress is correspondingly decreased even in a state of constant triaxiality of stress state. Thus, the critical length of remaining crack is decreased.

At very low temperature, as a microcrack is initiated, the normal stress is high enough to make it propagating unstably and the cleavage may be initiation controlled instead of propagation controlled.

## CONCLUSIONS

The critical event is changable from a notched to a precracked specimens for the same material and it is ferrite grain-sized microcrack propagating into neighboring grains for the notched specimens and second phase-sized microcrack into neighboring ferrite grains for the precracked specimens.

The variation of  $\sigma_f$  measured in notched and precracked specimens can be explained in terms of the different critical event of cleavage instead of the probabilistic effect of high stress volume.

The reason of variation of critical event in notched and precracked specimens may be attributed to the different sharpness at a notch root, which cause the variation of triaxiality and effective shear stress distribution below the notch.

## REFERENCES

- Chen, J. H et al. (1988). *Materials Science and Technology*, 4, 732.
- Chen, J. H et al. (1990a). *Met. Trans. A*, 21A, 313.
- Chen, J. H et al. (1990b). *Met. Trans. A*, 21A, 321.
- Chen, J. H et al. (1990c). *Acta. Metall*, 38, 2257.
- Chen, J. H et al. (1990d). *Unpublished*.
- Chen, J. H et al. *Met. Trans. A*, accepted
- Griffith, J. R et al. (1971). *J. Mech. Phys. Solids*, 19, 419.
- Hahn, G. H. (1984). *Met. Trans. A*, 15A, 947.
- Hou, C. X et al. (1985). 'Fracture 85', Proc. ICF6, 2, 14152, 1415
- Smith, E. (1966). The nucleation and growth of cleavage microcracks in mild steel. In: *Physical Basis of Yield and Fracture*, Institute of physics society, 1, 36.
- Stroh, A. N. (1957). *Adv. Phys*, 6, 418